DOI: 10.1002/chem.200500534

Environmental Effects on a Prion's Helix II Domain: Copper(II) and Membrane Interactions with PrP180–193 and Its Analogues

Domenico Grasso,[a] Giulia Grasso,[b] Valeria Guantieri,[c] Giuseppe Impellizzeri,[a] Carmelo La Rosa,[a] Danilo Milardi,[b] Giovanni Micera,[d] Katalin Õsz,[e] Giuseppe Pappalardo,[b] Enrico Rizzarelli,*[a, b] Daniele Sanna,[f] and Imre Sóvágó*[e]

Abstract: An abnormal interaction between copper and the prion protein is believed to play a pivotal role in the pathogenesis of prion diseases. Copper binding has been mainly attributed to the N-terminal domain of the prion protein, but this hypothesis has recently been challenged in some papers which suggest that the C-terminal domain might also compete for metal anchoring. In particular, the segment corresponding to the helix II region of the prion protein, namely PrP180–193, has been shown both to bind copper and to exhibit a copper-enhanced cytotoxicity, as well as to interact with artificial membranes. The present work is aimed at extending these results by choosing the most representative model of this domain and by determining its copper affinity. With this aim, the different role played by the electrostatic properties of the C- and N-termini of PrP180–193 (VNITIKQHTVTTTT) in determining its conformational behaviour, copper coordination and ability to perturb model membranes was investigated. Owing to the low solubility of PrP180–193, its copper affinity was evaluated by using the shorter PrPAc184–188NH_2 (IKQHT) analogue as a model. ESI-MS, ESR, UV/Vis, and CD measurements were carried out on the copper(II)/PrPAc184–188NH_2 and copper(II)/PrP180–193NH_2 systems, and showed that PrPAc184–188NH_2 is a reliable model for the metal interaction with the helix II domain. The affinity of copper(II) for the helix II fragment is higher than that for the octarepeat and PrP106–126 peptides. Finally, the different ability of PrP180–193 analogues to perturb the DPPC model membrane was assessed by DSC measurements. The possible biological consequences of these findings are also discussed briefly.

Keywords: copper · helical structures · membranes · peptides · prions

Introduction

Protein conformational diseases (PCDs) are characterised by the abnormal deposition of misfolded proteins. Among these pathologies, prion proteins (PrP) cause neurodegenerative diseases, including Creutzfeldt–Jakob disease (CJD), bovine spongiform encephalopathy (BSE), chronic wasting disease (CWD) and scrapie in mammals.[1] Prion pathologies are thought to be due to an altered isoform PrP^{Sc} of the normal protein PrP^{C}, which is converted into PrP^{Sc} through a process that does not involve any change in its primary structure.[2] The PrP^{C} protein is characterised by the pres-

[a] Prof. D. Grasso, Prof. G. Impellizzeri, Dr. C. La Rosa, Prof. E. Rizzarelli
Università di Catania, Dipartimento di Scienze Chimiche
Viale Andrea Doria 6, 95125 Catania (Italy)
Fax: (+39) 095-337-678
E-mail: erizzarelli@unict.it

[b] Dr. G. Grasso, Dr. D. Milardi, Dr. G. Pappalardo, Prof. E. Rizzarelli
Istituto CNR di Biostrutture e Bioimmagini – Sezione di Catania
Viale Andrea Doria 6, 95125 Catania (Italy)

[c] Prof. V. Guantieri
Università di Padova
Dipartimento di Chimica Inorganica, Metallorganica ed Analitica
Via F. Marzolo 1, 35131 Padova (Italy)

[d] Prof. G. Micera
Università di Sassari, Dipartimento di Chimica
via Vienna 2, 07100 Sassari (Italy)

[e] Dr. K. Õsz, Prof. I. Sóvágó
University of Debrecen
Department of Inorganic and Analytical Chemistry
4010 Debrecen (Hungary)
Fax: (+36) 52-489-667
E-mail: sovago@delfin.unideb.hu

[f] Dr. D. Sanna
Istituto CNR di Chimica Biomolecolare-Sezione di Sassari
Traversa La Crucca 3, Regione Baldinca, 07040 Li Punti (SS) (Italy)

ence of a flexible and "unstructured", roughly 100-residue N-terminal "tail" and a globular domain of nearly identical size which extends from residue 120 to residue 231 and is made up of two short antiparallel β-strands and three α-helices.[3,4] Although many efforts have been made, the function of the prion protein has not yet been identified, although several contributions have been reported on the key role of copper in the biology of PrP^C.[5] Investigations on copper binding to PrP^C have focused on the unstructured N-terminal segment of PrP, which contains four successive copies of the highly conserved octapeptide repeat sequence PHGGGWGQ.[6] Although there is agreement on the biological relevance of this metal binding region, the attribution of the primary location of the copper binding site and the structure of copper(II) complexes with the octapeptide ligand still remain a matter of debate, especially since contradictory results have been reported.[7–9] Preferential copper(II) coordination to an unstructured region of PrP encompassed between residues 90 and 115 has recently been suggested[9] by studying the competitive effect of the octarepeat domain on Cu^{2+} binding to the PrP91–115 fragment. Furthermore, the coordination of a single copper(II) ion to both His96 and His111 influences the structuring of this amyloidogenic region and induces a β-sheet-like conformation. These results reinforce the role of the metal ion in the well-known toxicity of the PrP106–126 peptide fragment.[10]

In addition to the copper(II) binding in the unstructured amyloidogenic region, it has been reported that Cu^{2+} coordinates to the structured C-terminal domain mPrP121–231, which contains three histidine residues, although spectroscopic approaches did not allow the determination of the coordination environment or the location of the binding sites of the three copper(II) complex species formed at different pHs.[11–13] A few studies have been carried out on copper(II) interactions with peptides in the domains of the three helices of PrP.[9,14] Among these, the peptide PrP178–193 (DCVNITIKQHTVTTTT), which corresponds to the helix II, has been found to promote copper(II)-induced lipid peroxidation and cytotoxicity in primary neuronal cultures, while the analogous PrP180–193 (VNITIKQHTVTTTT) forms amyloid, as evidenced by electron microscopy and Congo Red birefringence.[14] Interestingly, these peptides contain a histidine residue (His187), which can act as an anchoring binding site for copper(II) by means of its imidazole nitrogen.

More recently, the stoichiometry and the coordination modes of copper(II) with these two peptides were determined, both of which suggest the pivotal role played by the His187 residue as an anchoring site for the metal binding.[9] Herein, the ability of copper(II) to induce a conformational change in the secondary structure of the $PrPAc180–193NH_2$ peptide fragment (from α-helix to β-sheet) was also shown. However, the random coil conformation of PrP180–193 is not modified in the presence of the copper(II) ion. The different influence of the metal ion on the conformation features has been used to rationalize the significant increase of copper(II)-assisted $PrPAc180–193NH_2$ toxicity relative to the toxicity of unmodified PrP180–193.[9] The limited solubility of these PrP peptide fragments did not allow the determination of either their speciation or the stability constants of their metal complexes. On the other hand, a knowledge of the copper(II) affinity for this PrP region could help to assess the relevance of the helix II as a competitive copper(II) binding site with respect to both the PrP's N-terminus and the unstructured region between the octarepeats and the structured part of the prion protein (PrP106–126). In this work, initial attempts to measure the affinity of copper(II) for $PrPAc180–193NH_2$ were hindered by the low solubility of this fragment. To overcome this problem, an analogue of $PrPAc180–193NH_2$, the shorter and more-soluble $PrPAc184–188NH_2$ ($AcIKQHTNH_2$), was synthesised. This peptide, which contains the His 187 metal anchor site, is a good model for obtaining a reliable picture of the speciation, the affinity and the coordination environments of copper(II) complexes with the entire helix II domain. Potentiometric measurements were carried out (25 °C and $I = 0.2\ mol\,dm^{-3}$ KCl) to obtain the stability constants and the species distribution of the copper(II) complexes with this peptide fragment. The comparison of these stability constant values with those reported for copper(II) complexes with both the N-terminal octarepeat and the PrP106–126 peptide allowed us to determine the preferential binding site of copper(II) among these different protein regions. Furthermore, to investigate how the protection of the N-terminus and/or that of the C-terminus influences the conformational features and the metal binding properties of the PrP180–193 peptide, the N-terminally acetylated PrPAc180–193 and its C-terminally amidated analogue $PrP180–193NH_2$ were also synthesised. Owing to the low solubility of these partially protected fragments, the stoichiometries of their copper(II) complexes were determined by means of ESI-MS measurements. The coordination features of all copper(II) complexes were obtained by means of spectroscopic (UV/Vis, CD and EPR) measurements.

Association with biological membranes has also been suggested as an additional environmental factor that affects the conformational stability of PrP^C.[15] Such an effect may have important implications for the understanding of the mechanism associated with cell membrane damage caused by oligomeric intermediates identified in many PCDs.[16–19] Changes in membrane fluidity, permeability to ions, transient formation of lipid microdomains and variations of other membrane properties are manifestations of a general membrane-based cytotoxic mechanism that originates from an abnormal interaction with aggregation-prone polypeptides.[20] Prion is thought to be one of those aggregation-prone proteins that induce changes in membrane microviscosity and membrane rigidity.[21] Previous DSC experiments were carried out on different prion peptide fragments to simulate the interaction with biological membranes by using DPPC vesicles as model membranes. These investigations were performed both in the absence and in the presence of metal ions.[22–24] In this paper we report DSC results that show the ability of different PrP180–193 analogues to per-

meate phospholipid artificial membranes as well as the role of copper(II) in modulating this interaction.

Experimental Section

General: Peptide coupling reagents and peptide synthesis resins were purchased from Applied Biosystems. Amino acids were purchased from NovaBiochem. 1,2-Dipalmitoyl-sn-glycero-3-phosphocholine (DPPC) was obtained from Fluka. All inorganic salts for phosphate buffer preparation were purchased from Sigma.

Peptide synthesis: The peptide PrP180–193 and its N-terminally acylated/C-terminally amidated PrPAc180–193NH_2 (L_1), N-terminally acylated PrPAc180–193 and C-terminally amidated PrP180–193NH_2 derivatives, as well as the shorter fragment PrPAc184–188NH_2 (L) were synthesised by automated solid-phase peptide synthesis on a 431 A Applied Biosystems instrument. The synthesised peptides, assembled from Fmoc-protected amino acid derivatives, were cleaved from the solid support with a trifluoroacetic acid (TFA)/water/triethylsilane (95:2.5:2.5) mixture over the course of 3 h. All crude peptides were precipitated by concentration of the acid solution, resolubilised with a minimal quantity of TFA and then recrystallised twice from a methanol/diethyl ether mixture. The peptide-containing solutions were then injected into a Perkin-Elmer 410 HPLC system equipped with a LC-90UV detection system, with an aqueous acetonitrile gradient. An Aquapore RP-300 column was used. Amino acid analyses were carried out on a 3 A30 analyzer from Carlo Erba instruments. The purity was greater than 97% for all the peptides used.

Potentiometric measurements: The pH-potentiometric titrations were carried out with 3-mL samples in the concentration range 2×10^{-3} to 4×10^{-3} mol dm^{-3}, with metal ion to ligand ratios of between 1:2 and 2:1. During the titration, argon was bubbled through the samples to ensure the absence of both oxygen and carbon dioxide and also to mix the solutions. All titrations were performed at 298 K and at a constant ionic strength of 0.2 mol dm^{-3} (KCl) with a pH-meter Radiometer pHM84 equipped with a 6.0234.100 combination glass electrode (Metrohm) and a Dosimat 715 automatic burette (Metrohm) containing carbonate-free potassium hydroxide with a known concentration. The pH readings were converted into hydrogen ion concentration and protonation constants of the ligands, and the overall stability constants ($\log\beta_{pqr}$) of the complexes were calculated by means of a general computational program, PSEQUAD,[25] by using Equations (1) and (2).

$$pM + qL + rH = M_pL_qH_r \quad (1)$$

$$\beta_{pqr} = [M_pL_qH_r]/[M]^p \cdot [L]^q \cdot [H]^r \quad (2)$$

Spectroscopic measurements: Optical absorption spectra in the UV-Vis region were recorded at 25°C on a Varian UV-Vis Cary500 spectrophotometer using 1-cm path-length quartz cells. CD spectra were obtained at 25°C under a constant flow of nitrogen on a Jasco model J-810 spectropolarimeter calibrated with an aqueous solution of ammonium (1*R*)-(−)-10-camphor sulfonate.[26] Measurements were carried out in water or an H_2O/TFE (50%) mixture and at different pH values, in 1-mm or 1-cm path-length cuvettes. The CD spectra of the free peptide ligands were recorded in the UV region (190–260 nm), whereas those in the presence of Cu^{2+} were obtained in the wavelength ranges 190–380 and 380–750 nm. The spectra represent the average of 8–20 scans. All the solutions were freshly prepared in deionised water. The concentrations of the peptides and their copper(II) complexes used to record CD spectra in the UV region were 3×10^{-4} and 6.5×10^{-5} mol dm^{-3}, respectively, while a concentration of 1.0 mol dm^{-3} was used to obtain CD spectra of copper(II) complexes in the visible region (1:1 metal to ligand ratio). Due to the low water solubility of the PrP180–193NH_2 peptide, TFE was used as co-solvent to improve the signal to noise ratio, thus allowing good quality spectra to be obtained. The general spectroscopic profile was not affected by the co-solvent, as proved by comparison with the spectra recorded in water (data not shown).

Anisotropic X-band EPR spectra of frozen solutions were recorded at 120 K with a Bruker EMX spectrometer after addition of ethylene glycol to ensure good glass formation. The copper(II) stock solution for EPR measurements was prepared from $CuSO_4\cdot5H_2O$ enriched with ^{63}Cu to get better resolution of the EPR spectra. Metallic copper (99.3% ^{63}Cu and 0.7% ^{65}Cu) was purchased from JV Isoflex, Moscow, Russia, for this purpose and converted into the sulfate.

Electrospray mass spectrometry (ESI-MS) analysis: ESI-MS spectra were recorded with a Finnigan LCQ-Duo ion trap electrospray mass spectrometer (Bremen, Germany). Peptide solutions were introduced into the ESI source through 100-μm i.d. fused silica from a 250-μL syringe. The experimental conditions for spectra acquired in positive ion mode were as follows: needle voltage: 2.5 kV; flow rate: 5 μL min^{-1}; source temperature: 150°C; *m/z* range: 200–2000; cone potential: 46 V; tube lens offset: −34 V. The experimental conditions for spectra acquired in negative ion mode were as follows: needle voltage: 2.5 kV; flow rate: 5 μL min^{-1}; source temperature: 150°C; *m/z* range: 200–2000; cone potential: −10 V; tube lens offset: 16 V.

The complexes were prepared by dissolving the peptide and $CuSO_4$ (5×10^{-5} mol dm^{-3}) in Milli-Q water at a 1:1 metal to ligand ratio and were investigated in the pH range 4.5–9.5, adjusting the pH values by adding HCl or NaOH.

Because of the isotopic distribution of elements, molecular species were detected in the mass spectra as clusters of peaks, so, to simplify their attribution, the *m/z* values indicated in the spectra and in the text correspond to the first (lowest-mass) peak of each cluster. In the formulae reported in the text, the substitution of hydrogen atoms of the peptides with copper atoms is indicated in brackets. For example, $[PrP180–193+Cu-2H]H^+$ indicates a peptide molecule in which two H atoms have been substituted by a Cu atom. In all cases the cationizing agents are placed outside the brackets and their charge is indicated. Other details are as reported previously.[27,28]

Preparation of large unilamellar vesicles (LUV): Model membranes were prepared as described elsewhere.[22] Briefly, solutions of pure phospholipids in $CHCl_3$ were dried under nitrogen and evaporated to dryness under high vacuum in round-bottomed flasks. The resulting lipid film on the wall of the flask was hydrated with an appropriate volume of buffer and dispersed by vigorous stirring in a water bath set at 4°C above the gel–liquid crystal transition temperature of the membrane. The final nominal concentration of the lipid was 2 mg mL^{-1}. In order to obtain large unilamellar vesicles (LUV), the multilamellar vesicles thus obtained were extruded through polycarbonate filters (pore size = 100 nm) (Nuclepore, Pleasanton, CA) mounted in a mini-extruder (Avestin Inc.) fitted with two 0.5-mL Hamilton gastight syringes (Hamilton, Reno, NV). Samples passed 19 times through two filters in tandem, as recommended elsewhere.[22] An odd number of passages were performed to avoid contamination of the sample by vesicles that might not have passed through the filter. Two different protocols were applied to prepare mixed lipid/peptide bilayers: a) the peptide fragment was dissolved in the same organic solution ($CHCl_3$) as the phospholipid (peptide/lipid molar ratio of 1/10), and then extruded according to the procedure above described; b) an appropriate amount of peptide was added to the previously prepared DPPC LUV suspension to give a final peptide/lipid molar ratio of 1/10. The mixture was initially vigorously vortexed for 1–2 min and then, unless otherwise specified, immediately scanned.

Differential scanning calorimetry: DSC scans were carried out with a second-generation high-sensitivity SETARAM micro differential scanning calorimeter (microDSC II) with 1-mL stainless-steel sample cells, interfaced with a BULL 200 Micral computer. The sampling rate was one point per second in all measuring ranges. The same solvent without the sample was used in the reference cell. Both the sample and reference were heated with a precision of 0.05°C at a scanning rate of 0.5°C min^{-1}. To obtain the excess heat capacity (Cp_{exc}) curves, buffer–buffer baselines were recorded at the same scanning rate and then subtracted the from sample, as described previously.[22] Energy calibration was performed by providing a definite power supply, electrically generated by an EJ2 SETARAM Joule calibrator within the sample cell. To check the reproducibility of the results, three different samples were scanned. In the case of

DPPC model membranes only the main transition was considered because the pre-transition is strongly dependent on the preparation method of the membrane and it disappears when the liposomes are extruded.[29] All DSC experiments were repeated after 24 and 48 h, but no kinetic effects were ever observed.

Results and Discussion

Copper(II) complexes: stability, binding sites and induced conformation features: To determine the different complex species formed by copper(II) with the PrPAc180–193NH_2 protein fragment, the speciation of the copper(II) complexes with the short and soluble analogue PrPAc184–188NH_2 was determined from potentiometric measurements. A comparison between the potentiometric and ESI-MS results allowed the validation of the pentapeptide as a model system.

Only mononuclear complex species were found. Bis-complexes were rejected on the basis of computer calculations, even in the presence of an excess of peptide with respect to copper(II) (1:3 metal to ligand ratio).

Table 1 shows the stability constant values of proton and copper(II) complexes with PrPAc184–188NH_2. The pentapeptide has two protonation sites, namely the imidazole nitrogen atom of His187 and the ε-amino group of Lys185.

Table 1. Equilibrium data for the copper(II) complexes with PrPAc184–188NH_2 (L) ($I=0.2$ mol dm^{-3} KCl, $T=298$ K).

Species	log β	pK
HL	6.29(1)	(His) 6.29(1)
H_2L	16.56(1)	(Lys) 10.27(1)
CuLH	14.01(2)	
$CuLH_{-1}$	2.40(1)	
$CuLH_{-2}$	−5.88(2)	
$CuLH_{-3}$	−16.04(2)	
		(Cu-Lys) 10.16(2)

The protonation constant of the imidazole nitrogen atom is in good agreement with those of other histidine-containing peptides. Deprotonation of the lysyl amine group takes place above pH 10, and the value corresponds well to that found for other peptides containing lysine residues.[30] Figure 1 shows that the complex formation starts with the formation of the monoprotonated species $[CuLH]^{3+}$. The log$K$ value (3.74) is similar to that reported for a copper(II) monoimidazole complex, thus showing that the peptide binds to the metal ion through the imidazole nitrogen of histidine, with the lysine remaining protonated. The EPR parameters, collected in Table 2, are close to those reported for copper(II) complexes in which the metal is bound to an imidazole nitrogen,[31–34] thus confirming the monodentate binding of the His residue. The formation of the species $[CuLH_{-1}]^{+}$ from $[CuLH]^{3+}$ takes place in a cooperative manner. This reaction is characterised by a significant blue shift of the absorption spectra (Figure 2), as expected for the deprotonation and coordination of two amide groups,

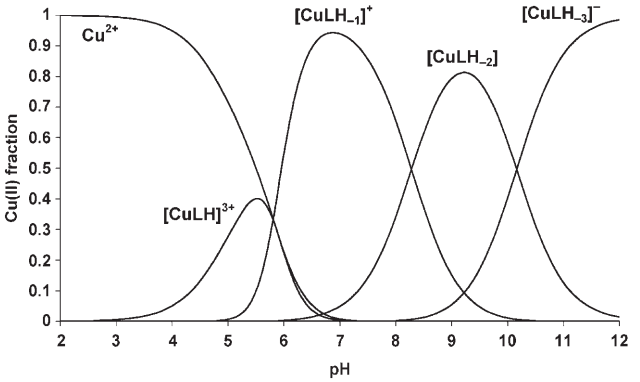

Figure 1. Species distribution of the complexes formed in the copper(II)/PrPAc184–188NH_2 (L) system at a 1:1 copper(II) to ligand ratio: $C_{PrPAc184-188NH_2}=2.0\times10^{-3}$ mol dm^{-3}; $C_{Cu^{II}}=1.9\times10^{-3}$ mol dm^{-3}.

Table 2. Spectroscopic parameters of copper(II) complexes with PrPAc184–188NH_2 (L) and PrPAc180–193NH_2 (L_1)[9]

Species	UV/Vis λ [nm] (ε [M^{-1}cm^{-1}])	CD λ [nm] ($\Delta\varepsilon$ [M^{-1}cm^{-1}])	EPR $g_{\parallel}$ ($A_{\parallel}$ [10^{-4} cm^{-1}])
CuLH	–	520 (+0.280), 337 (−0.385)	2.358 (151)
$CuLH_{-1}$	600 (91)	604 (−0.062), 520 (+0.387), 341 (−0.615)	2.229 (172)
CuL_1H_{-1}	586 (80)	591 (−0.106), 523 (+0.331), 346 (−0.661), 298 (+0.506), 254 (+4.372)	2.230 (172)
$CuLH_{-2}$	512 (133)	643 (+0.631), 494 (−1.10), 354 (−0.440), 294 (+0.919)	2.185 (196)
CuL_1H_{-2}	519 (100)	639 (+0.513), 490 (−0.911), 355 (−0.586), 307 (+1.482), 256 (+6.013)	2.184 (200)
$CuLH_{-3}$	512 (136)	645 (+0.642), 497 (−1.112), 356 (−0.449), 294 (+0.887)	2.185 (196)

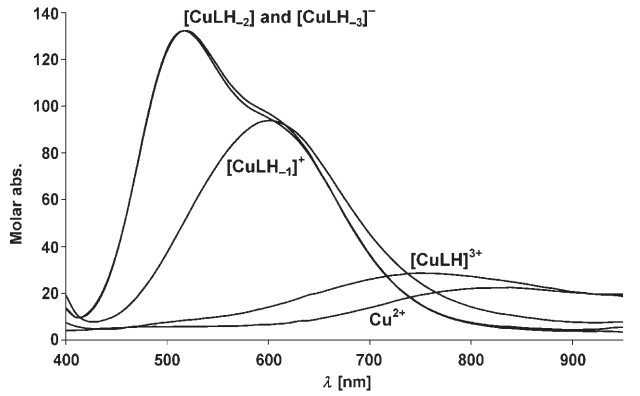

Figure 2. Molar absorption spectra of the species formed in the copper(II)/PrPAc184–188NH_2 (L) system. The spectra were calculated with the program PSEQUAD.

most probably the His187 and the Gln186. The CT bands in the CD spectra due to $N_{im}\rightarrow Cu^{2+}$ and $N^{-}\rightarrow Cu^{2+}$ indicate that $[CuLH_{-1}]^{+}$ is a 3N complex with an (N_{im}, 2× N(amide)$^{-}$) coordination mode, while the amine group of

lysine is still protonated. In fact, the stoichiometry of the species is $[CuLH_{-1}]^+ = [Cu(LH_{-2})H]^+$. The $g_\parallel$ and $A_\parallel$ values (Table 2) are similar to those reported for similar species of copper(II) complexes with prion octarepeat fragments.[35] A further increase of pH results in changes to all the spectral parameters, most notably a blue shift of the d–d transitions in the absorption spectra, a shift and inversion of the sign of the CD band at 495 nm, an increase of the intensity of the band at 640 nm and formation of a new band at 294 nm (Figure 3). These spectral changes indicate the deprotonation of a third amide residue (Lys185), resulting in the formation of a 4N complex with a different disposition of the imidazole residue, as indicated by the CD parameters and the $g_\parallel$ and $A_\parallel$ values (Table 2). Deprotonation of the lysyl side-chain takes place in the same pH range as for the free ligand (pH > 10). This deprotonation reaction is, however, not accompanied by any spectral changes (Table 2 and Figure 4), which indicates that the ε-amine group is not a metal binding site at any pH value. The equilibrium data confirm this conclusion because the protonation constants of the copper(II) complex and the free ligand (see pK_{Cu-Lys} and pK_{Lys} values in Table 1) are almost the same. In addition, the spectroscopic parameters of copper(II) complexes with PrPAc184–188NH_2 are very similar to those previously reported[9] for the analogous species formed by copper(II) with PrPAc180–193NH_2.

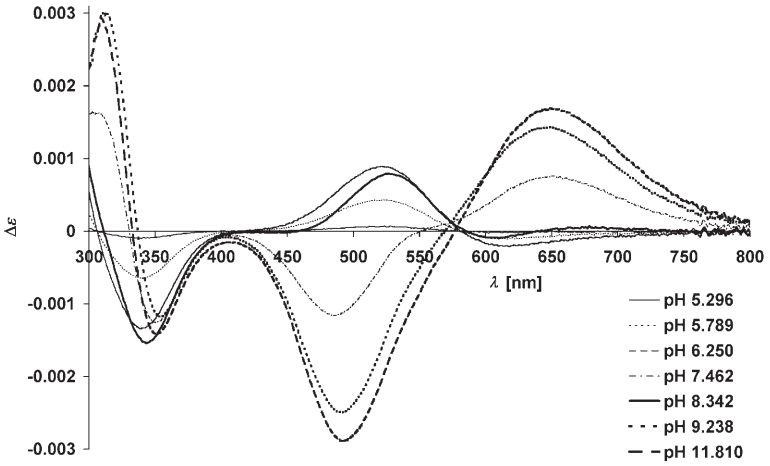

Figure 3. CD spectra measured in the copper(II)/PrPAc184–188NH_2 (L) system at a 1:1 copper(II) to ligand ratio: $C_{PrPAc184-188NH_2} = 1.9 \times 10^{-3}$ mol dm^{-3}; $C_{Cu^{II}} = 1.8 \times 10^{-3}$ mol dm^{-3}.

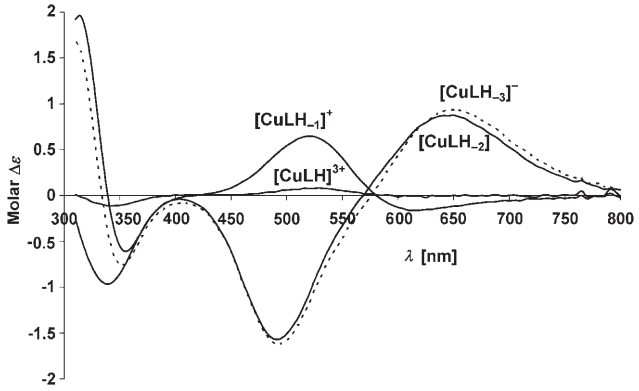

Figure 4. Molar CD spectra of the species formed in the copper(II)/PrPAc184–188NH_2 (L) system. The spectra were calculated with the program PSEQUAD.

The ESI mass spectrum of a PrPAc184–188NH_2 solution shows peaks at *m/z* 667.5, 690.3 and 335.1 (assigned as $[PrPAc184–188NH_2]H^+$, $[PrPAc184–188NH_2]Na^+$ and $[PrPAc184–188NH_2]H_2^{2+}$, respectively). Upon adding copper(II) sulfate, peaks attributed to the copper(II)–peptide complexes at *m/z* 375.7 ($[PrPAc184–188NH_2+Cu-2H]H_2^{2+}$), 728.4 ($[PrPAc184–188NH_2+Cu-2H]H^+$), 750.6 ($[PrPAc184–188NH_2+Cu-2H]Na^+$)and 766.2 ($[PrPAc184–188NH_2+Cu-2H]K^+$) appear, in addition to some signals due to the uncomplexed peptide (Figure 5). The ESI mass spectrum at pH 9.5, obtained in the negative mode, shows a signal at *m/z* 726.3 attributed to $[PrPAc184–188NH_2+Cu-3H]^-$. The stoichiometry of the copper(II) complexes with the pentapeptide obtained by ESI-MS is in agreement not only with the speciation determined by potentiometry, but also with that previously reported for the copper(II) complexes formed with PrPAc180–193NH_2,[9] thus indicating that PrPAc184–188NH_2 is a reliable model for studying the affinity of copper(II) for the PrP helix II domain.

The ESI mass spectrum of the prion fragment PrPAc180–193 only shows peaks at *m/z* 1598.5, 1620.5, 800.1 and 811.1, assigned as $[PrPAc180–193]H^+$, $[PrPAc180–193]Na^+$, $[PrPAc180–193]H_2^{2+}$ and $[PrPAc180–193]HNa^{2+}$ respectively. The spectra recorded in the presence of copper(II) sulphate reveal only the peaks ascribable to uncomplexed PrPAc180–193 ligand due to the aggregation tendency of this peptide. The ESI mass spectrum of PrP180–193NH_2 shows peaks at *m/z* 1555.6, 1577.5, 778.7 and 790.1, assigned as $[PrP180–193NH_2]H^+$, $[PrP180–193NH_2]Na^+$, $[PrP180–193NH_2]H_2^{2+}$ and $[PrP180–193NH_2]Na_2^{2+}$, respectively. In the presence of an equimolar amount of copper(II) sulfate, the formation of copper(II) complexes occurs and the spectrum shows peaks at *m/z* 809.7, 1616.7, 820.7 and 831.7 for $[PrP180–193NH_2+Cu-2H]H_2^{2+}$, $[PrP180–193NH_2+Cu-2H]H^+$, $PrP180–193NH_2+Cu-2H]HNa^{2+}$ and $[PrP180–193NH_2+Cu-2H]Na_2^{2+}$, respectively. The ESI mass spectrum at pH 8.5, obtained in the negative mode, shows signals at *m/z* 1589.4, 1614.5 and 1650.3 for $[PrP180–193NH_2]Cl^-$, $[PrP180–193NH_2+Cu-3H]^-$ and $[PrP180–193NH_2+Cu-2H]Cl^-$, respectively.

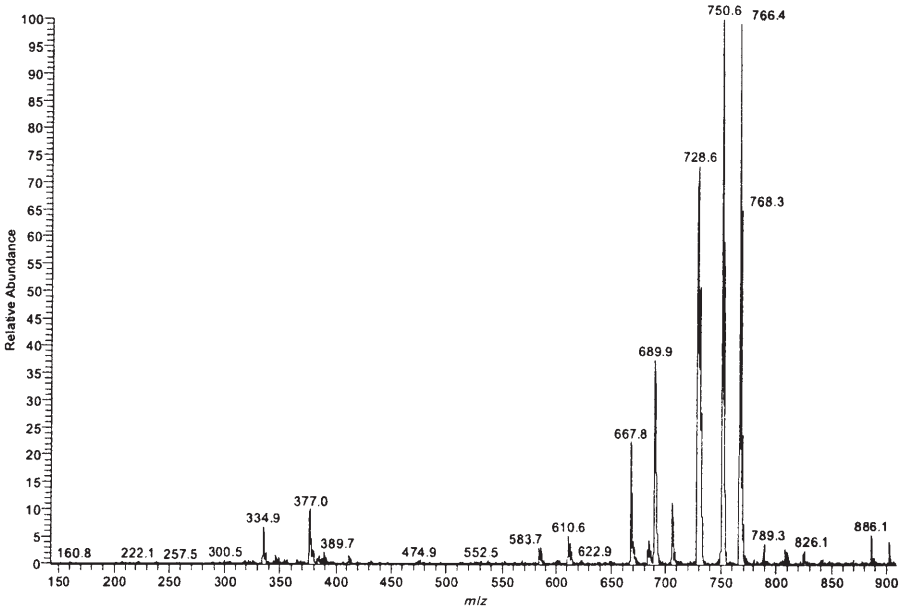

Figure 5. ESI positive-ion mass spectrum of a 1:1 PrPAc184–188NH_2/Cu^{II} system at pH 7.

The stoichiometries of the copper(II) complexes with the C-amidated peptide are the same as those of the previously reported N- and C-terminally blocked PrPAc180–193NH_2 and those with the short peptide fragment PrPAc184–188NH_2. For these peptides, only histidine can act as an anchoring site. PrP180–193NH_2, however, has two potential binding sites: the amine and the imidazole nitrogens. At pH 5.0, the λ_{max} of the absorption spectrum and the $g_{\parallel}$ and $A_{\parallel}$ values (Table 3) are similar to those reported for two nitrogen donor atoms in similar systems;[36] the CD bands at 270 and 306 nm due to $NH_2 \rightarrow Cu$ and $N^- \rightarrow Cu$ CT transitions, respectively, clearly show the involvement of both the amine N-terminus and a deprotonated amide nitrogen in the coordination of the metal ion. The increase of pH is accompanied by a blue shift of λ_{max} in the absorption spectrum and by the presence of the diagnostic CD signal of an $N_{im} \rightarrow Cu$ CT band at 325 nm. In addition, the CD band at 270 nm disappears (Table 3), which indicates that the anchoring site is now the histidine residue; at the same time, the $g_{\parallel}$ value decreases and becomes similar to that reported for the copper(II) complex of the prion octarepeat, for which a species with a 3N (N_{im}, $2\times N^-$) coordination mode has been reported.[34,35] The decrease of λ_{max} and the increase of the ε value suggest that copper(II) induces a distortion of the octahedral geometry, as found for the above-cited complexes with the octapeptide. It is noteworthy that, overall, the spectroscopic parameters are similar to those found for the $[CuLH_{-1}]$ species of PrPAc184–188NH_2. At basic pH values, a further blue shift of the d–d band is observed in the absorption spectrum, while the CD spectrum (Table 3) is characterised by changes very similar to those reported for the $[CuL_1H_{-2}]$ species of the pentapeptide analogous to PrPAc180–193NH_2 (see Table 2). This similarity is also underlined by similar EPR parameters, showing that a 4N complex is again formed.

Table 3. Spectroscopic parameters of copper(II) complexes with PrP180–193NH_2 (L_1, 50% TFE/water mixtures).

pH	UV λ [nm] (ε [$M^{-1}cm^{-1}$])	CD λ [nm] ($\Delta\varepsilon$ [$M^{-1}cm^{-1}$])	EPR $g_{\parallel}$ ($A_{\parallel}$ [10^{-4} cm^{-1}])
5	619 (82)	660 (−0.207)	2.238 (187)
		306 (−0.143)	
		270 (+0.263)	
7	600 (116)	676 (−0.455)	2.228(175)
		519 (+0.209)	
		325 (+0.317)	
		257 (+4.712)	
11	515 (144)	677 (+0.115)	2.180 (205)
		549 (−1.222)	
		497 (−1.278)	
		314 (+1.459)	
		256 (+7.617)	

In the UV region, the CD spectra of PrPAc184–188NH_2 show a random coil conformation in the whole pH range investigated (Figure 6a). Conversely, copper(II) influences the CD spectra of PrPAc184–188NH_2 (Figure 6b) depending on the pH. At pH 5, a negative band at about 198 nm is observed, consistent with the persistence of a random coil conformation. The CD curves recorded above pH 6 are characterised by the inflection of the negative signal at 218 nm, which is accompanied by a decrease of the band at 198 nm; the peptide chain appears to be more structured, probably toward a β-turn structure. At pH 9, the spectrum shows a positive band at about 205 nm and a negative one at 218 nm. Such a spectral pattern has often been associated with a type II β-turn conformation.[37] Analogously to what is observed with PrPAc184–188NH_2, the CD spectra of the longer peptide PrP180–193NH_2 indicate the presence of a random coil conformation in the entire pH range investigated (data not shown). Upon metal addition to PrP180–193NH_2, the CD curves show changes associated with a decreased negative ellipticity at 198 nm as a function of the increasing pH (Figure 7a).

The difference spectra obtained by subtracting the CD spectra of PrP180–193NH_2 from those of PrP180–193NH_2/Cu^{II} are shown in Figure 7b. The resultant CD curves show a similar trend to the PrPAc184–188NH_2/Cu^{II} system reported above, confirming again the reliability of this fragment as a representative model of the helix II domain.

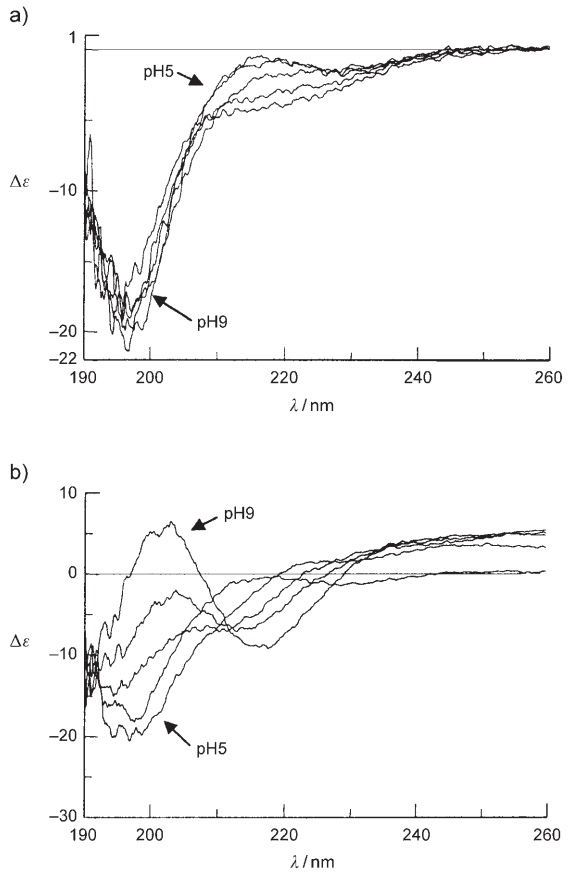

Figure 6. a) CD spectra of aqueous solutions of PrPAc184–188NH_2 (5×10^{-5} mol dm^{-3}) at different pH values. b) CD spectra of aqueous solutions of PrPAc184–188NH_2/Cu^{II} (5×10^{-5} mol dm^{-3}) at different pH values.

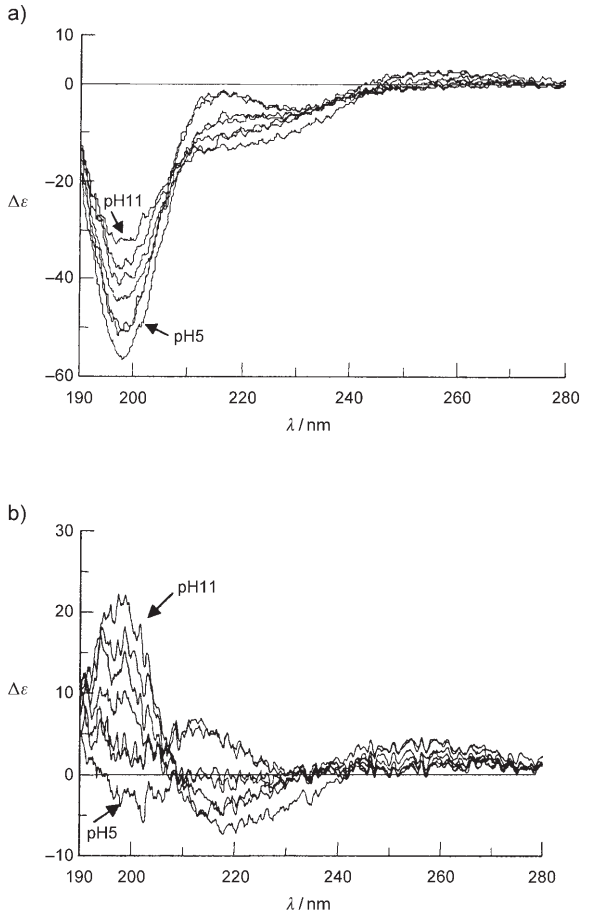

Figure 7. a) CD spectra of aqueous solutions of PrP180–193NH_2/Cu^{II} (5×10^{-5} mol dm^{-3}) at different pH values. b) CD difference spectra of PrP180–193NH_2.

Copper(II) binding affinity: comparison of the different regions of PrP: There is much interest in copper(II) binding affinity to the different regions of PrP^C. The recently reported stability constants of copper(II) complexes with the octarepeat-containing peptides[8,38,39] and a polar fragment (PrPAc106–114NH_2) of the unstructured PrP106–126 region,[40] as well as the complex formation constants concerning the structured helical II domain, facilitate a quantitative description of the tendency of a metal ion to interact with different parts of the protein.

The distribution diagrams reported in Figure 8 and Figure 9 were used to compare the metal binding affinity of the three different regions of the protein. It is clear from these figures that copper(II) binding of imidazole residues of the octarepeat monomer and His111 and His187 starts above pH 4 in all three segments of the protein, with the monodentate imidazole coordination being the major process in slightly acidic solutions. However, significant differences can be observed in the metal binding affinity upon increasing pH, thus suggesting different tendencies in the metal ion coordination ability of the amide function. Figure 8 reveals that the overall metal binding capacity of the nonapeptide PrPAc106–114NH_2 (Ac-KTNMKHMAG-NH_2) is very similar to that of the pentapeptide PrPAc184–188NH_2. For the 3N complexes with (N_{Im}, $2\times N^-$) coordination, the pentapeptide seems to be slightly favoured over the nonapeptide (see the concentration of the species

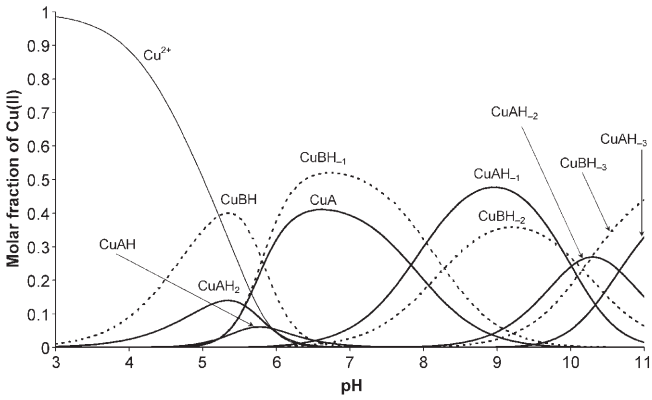

Figure 8. Distribution diagram of the copper(II) complexes formed in the Cu^{II}/PrPAc106–114NH_2 (A)/PrPAc184–188NH_2 (B) systems at a 1:1:1 ratio ($C_{Cu^{II}}=C_{PrPAc106-114NH_2}=C_{PrPAc184-188NH_2}=4\times10^{-3}$ mol dm^{-3}). Copper(II)/PrPAc106–114NH_2 (A) complexes are indicated by continuous lines and copper(II)/PrPAc184–188NH_2 (B) complexes are indicated by broken lines.

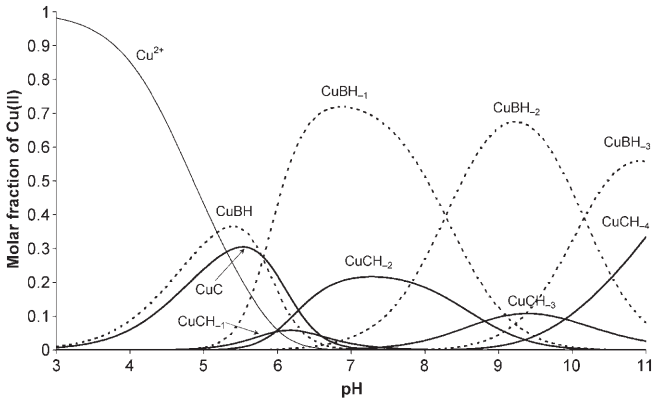

Figure 9. Distribution diagram of the copper(II) complexes formed in the Cu^{II}/octarepeat (C)/PrPAc184–188NH_2 (B) system at a 1:1:1 ratio: $C_{Cu^{II}} = C_{octarepeat} = C_{PrPAc184-188NH_2} = 4 \times 10^{-3}$ mol dm^{-3}. Copper(II)/octarepeat (C) complexes are indicated by continuous lines and copper(II)/PrPAc184–188NH_2 (B) complexes are indicated by broken lines.

[$CuBH_{-1}$] versus [CuA]) while it is the opposite for the 4N complex ([$CuAH_{-1}$] versus [$CuBH_{-2}$]). These small differences suggest that the two peptide fragments have the same coordination mode, although the overall thermodynamic stability is also influenced by the different charges of the complexes and by the non-coordinating side-chain residues. On the other hand, it is obvious from Figure 9 that the metal binding affinity of the octarepeat is significantly lower than that of the penta- or nonapeptides. The formation of both 3N and 4N complexes is favoured for the pentapeptide over the octarepeat monomer (see [$CuBH_{-1}$] and [$CuBH_{-2}$] versus [$CuCH_{-2}$] and [$CuCH_{-3}$]). The ratio of the complexed forms of the pentapeptide and the octarepeat monomer is around 4:1 above a pH of about 7. The dominant metal binding capacity of PrPAc106–114NH_2 and PrPAc184–188NH_2 over the octarepeat monomer probably comes from the differences in the chelate ring size: deprotonation and metal ion coordination of the amide function occurs towards the N-termini in the form of (6,5,5)-membered chelates for PrPAc106–114NH_2 and PrPAc184–188NH_2, whereas the presence of proline in the octarepeat sequence addresses the metal ion coordination of amide functions towards the C-terminus and (7,5,5)-membered chelates are formed. The thermodynamic stability of a seven-membered chelate is always lower than that of six-membered ones, and this is reflected in the reduced metal binding affinity of the octarepeat monomers.

Peptide interactions with artificial membranes: The combined use of DSC and CD investigations permitted us to correlate peptide-induced membrane perturbations and conformational features of the guest peptides. In fact, it is possible to relate the decrease of the transition enthalpy of the bilayer with the extent of the interaction between the guest molecules and the hydrophobic tails of the lipid membranes.[41] Analogously, the gel–liquid crystal transition temperature (T_m) of DPPC vesicles is more indicative of interactions that involve the head groups: in particular, it has been shown[23] that T_m changes depending on the increase of interactions in the interfacial region. An analysis of the calorimetric profiles of all the investigated DPPC/prion peptide systems has shown that the thermally induced transition of the DPPC membrane is affected differently by the peptides and also depends on the sample-preparation protocol according to the two experimental procedures reported in the Experimental Section (Figure 10). Table 4 lists the temperature transitions (T_m) and enthalpy changes (ΔH) concerning the lipid/peptide systems investigated. In particular, according to the preparation method b), PrPAc180–193 and PrP180–193NH_2 interact with the interfacial region of the bilayer, as evidenced by the increase in T_m. The lipid tails are not involved in this kind of interaction as the ΔH of the DPPC transition is only slightly modified by the presence of the peptides. On the contrary, according to the experimental protocol a), these two peptides interact differently with the membrane: PrP180–193NH_2 induces a dramatic reduction in the ΔH of the DPPC transition, thus suggesting an effective perturbation of the lipid tails of the hydrophobic core, whilst PrPAc180–193 increases the T_m of the gel–liquid crystal transition of the DPPC bilayer, probably due to an interaction with the interfacial region. These results suggest that the specific interaction with the membrane depends on the fragment investigated, and, in particular, on the distribution and presence of charges. In order to study the effect of the

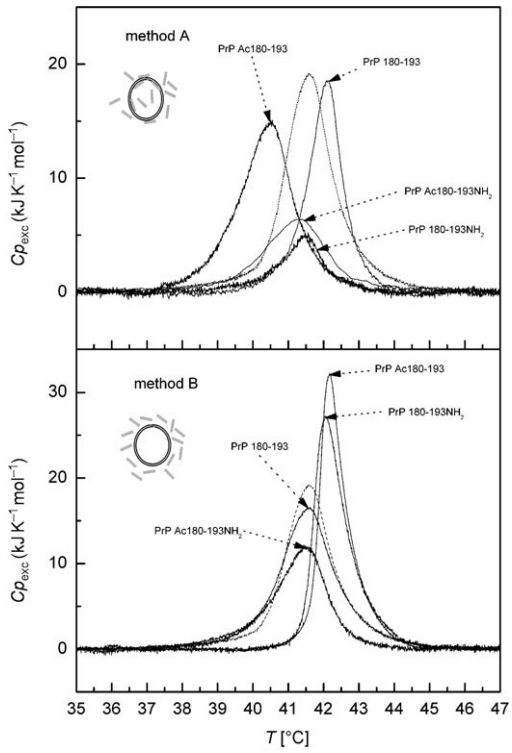

Figure 10. DSC curves for mixtures of PrP180–193/DPPC, PrPAc180–193NH_2/DPPC (taken from ref.[24]), PrPAc180–193/DPPC and PrP180–193NH_2/DPPC (this work). The lipid dispersions were prepared according to methods a (upper panel) and b (lower panel; see Experimental Section). Dotted lines represent the DSC transition of a pure DPPC model membrane prepared according to the same protocol as a control.

Table 4. Calorimetric peak temperatures (T_m) and total enthalpy changes (ΔH) relative to the different peptide/lipid bilayer systems.[a]

Method of preparation	DPPC		DPPC/PrP180–193		DPPC/PrPAc180–193NH_2		DPPC/PrPAc180–193		DPPC/PrP180–193NH_2	
	T_m [°C]	ΔH [kJ mol^{-1}]	T_m [°C]	ΔH [kJ mol^{-1}]	T_m [°C]	ΔH [kJ mol^{-1}]	T_m [°C]	ΔH [kJ mol^{-1}]	T_m [°C]	ΔH [kJ mol^{-1}]
a)	41.61 ± 0.02	36.0 ± 1.2	42.13 ± 0.02	24.8 ± 1.2	41.31 ± 0.01	16.2 ± 1.3	40.50 ± 0.01	30.2 ± 1.0	41.55 ± 0.01	8.4 ± 1.1
b)	–	–	41.58 ± 0.02	36.2 ± 1.0	41.50 ± 0.02	23.1 ± 1.1	42.16 ± 0.02	33.3 ± 0.9	42.03 ± 0.02	33.5 ± 1.2

[a] Experimental values are reported as mean ± standard deviation of three repeated experiments. Data for the DPPC/PrP180–193 and DPPC/PrPAc180–193NH_2 systems are taken from the literature.[24]

membrane environment on the conformational features of all PrP180–193 analogues, CD spectra were recorded on the lipid/peptide systems. However, due to the high level of scattering exhibited by LUVs, these systems had to be sonicated to obtain small unilamellar vesicles (SUV) as described in the Experimental Section. The CD spectra (Figure 11) show that the conformation of all studied peptides is essentially β-sheet. These results are in agreement with thermodynamic models, which show that the driving force of the incorporation of a peptide into the lipid bilayer is generally dominated by the unfavourable free-energy cost of inserting the peptide bonds into the hydrocarbon core (5 kJ mol^{-1} per peptide bond).[42] However, if the peptide in the lipid matrix adopts a structure that forms H-bonds, it can reduce this high free-energy cost. Thus, the formation of α-helices or β-sheets can promote the incorporation of a peptide into a hydrocarbon environment. All the DPPC/peptide systems investigated were also titrated with increasing amounts of copper(II), changing the peptide/metal ratio from 1 to 6. DSC analysis showed that only the DPPC/PrP180–193 system[24] was influenced by copper(II). This result is consistent with the hypothesis that the PrPAc180–193 or PrP180–193NH_2 fragments are also inserted into the membrane, thereby hampering the copper(II)–histidine interaction.

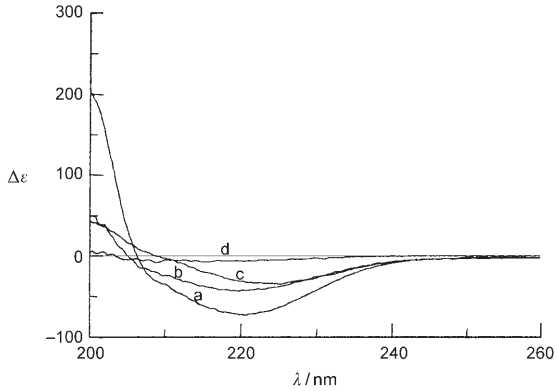

Figure 11. CD spectra of a) PrP180–193, b) PrPAc180–193, c) PrP180–193NH_2 and d) PrPAc180–193NH_2 at a concentration of 2.9×10^{-4} mol dm^{-3} and pH 7 in DPPC mixtures.

It is now generally accepted that the environment strongly affects the properties of PrP^C and its fragments, as well as the properties of the other proteins involved in amyloid diseases. In particular, it has been reported that interactions with metal ions[43] and membranes[20] modify the biological functions of these proteins.[44] As concerns the copper(II) complexes with PrP^C, a large number of studies have addressed the characterisation of the four copper ions binding to the octarepeat region. However, only recent results have allowed the identification of the different species formed by this metal ion with the mono-, bis- and tetraoctapeptides of the N-terminal region in the physiological pH range.[38,39] The related stability constant values were obtained by means of potentiometric or spectroscopic measurements, thus clarifying the previously conflicting affinity data with reported K values between the micromolar and femtomolar range.[8] Although additional binding sites have been discovered involving either the unstructured domain between the N-terminal region and the structured domain or the α-helical region, only the speciation of complexes involved in the copper binding to PrP106–126, which encompasses the unstructured domain, and the related stability constant values have been reported.[5,45] In this latter case, the use of the PrP106–126 peptide fragment with its N-terminus unblocked might not be fully representative of this part of the PrP^C protein. In fact, copper(II) binds to the N-terminal amino nitrogen at position 106, a donor atom that is not present in the protein chain. More recently, preferential copper(II) coordination by His96 and His111 has been reported, but neither the speciation of metal complexes nor the related stability constants were determined.[46] The present results show that PrPAc184–188NH_2 and, consequently, PrPAc180–193NH_2 bind a single copper(II) more tightly than both the octarepeat region and the peptide fragment PrP106–126. EPR data for copper(II) complexes with full-length mPrP23–231, its C-terminal domain mPrP121–231 and the N-terminal fragment[47,48] (Table 5) have been reported and three different copper(II) species have been detected in the pH range 3–8. It was suggested that complexes **1** (existing in the pH range 3–6) and **2** (formed in the pH range 3–8) are related to the C-terminal part of mPrP121–231, while complex **3** shares spectroscopic features with copper(II) containing mPrP23–231, mPrP121–231 and mPrP58–91 at physiological pH values.[11] Interestingly, the EPR parameters of PrPAc184–188NH_2 are close to those previously reported for the above-mentioned copper(II) complex **3**. The pentapeptide is therefore a reliable model, stressing the role of His187 as a binding site for this structured region of PrP. Furthermore, the combined use of potentiometry and ESI-MS enables the determination of the stoichiometry and the

Table 5. EPR parameters of the copper(II) complexes with mPrP23–231, mPrP121–231 and mPrP58–91 fragments of prion protein and some peptide fragments at physiological pH.

Protein/Peptide fragments	$g_{\parallel}$	$A_{\parallel}$ [10^{-4} cm^{-1}]	Ref.
mPrP23–231	2.230	165	[11]
mPrP121–231	2.230	165	[11]
mPrP58–91	2.230	165	[11]
AcPHGGGWGQNH$_2$	2.230	166	[47]
AcPHGGGWGQNH$_2$	2.235	160	[48]
PrPAc180–193NH$_2$	2.230	172	[9]

speciation of metal complexes, thus showing that [CuLH$_{-1}$] is the main metal complex species formed by the different protein domains in the physiological pH range.

Moreover, several experimental observations strongly support the hypothesis that an abnormal interaction of PrP with the lipid membrane might be involved in the process of its conversion into PrP^{Sc}.[19,20] To gain insight into this issue, in vivo and in vitro studies have been carried out[21–24] using synthetic segments of the prion protein corresponding to regions believed to interact with membranes. In the same papers, the formation of aggregated forms of the peptide has been suggested in the membrane, and this underlines the specific role of the electrostatic interactions and of copper in modulating the lipid/peptide interactions.[24] Here, PrPAc180–193/DPPC and PrP180–193NH$_2$/DPPC systems were used to explore the role of copper(II) binding and membrane interactions in affecting the secondary structure of the helix II prion domain. The comparison between the DSC results of DPPC/PrPAc180–193 and DPPC/PrP180–193NH$_2$ with those of DPPC/PrP180–193 and DPPC/PrPAc180–193NH$_2$ shows that the features of the N- and C-termini greatly influence both the copper binding and the ability of the peptides to interact with the membrane. Although it is necessary to be cautious in extending the results obtained with peptide fragments to wild-type proteins, the DSC results for different PrP180–193 analogues clearly indicate the need to choose peptides with the C- and N-termini blocked as reliable model analogues.

The possible biological consequences of the findings reported in the present paper may be relevant. The number of studies aimed at investigating the inherent toxicity of the C-terminal domain and related fragments has increased, and they are in agreement that the N-terminus (amino acid residues 23–90) is not associated with disease.[46] Shmerling et al.[49] have shown that mice expressing a PrP^{C} fragment (PrP121–231) die within several weeks after birth due to massive neurodegeneration in the granule cell layer of the cerebellum. Furthermore, addition of a peptide encompassing the amino acid residues 112–125 to cerebellar cultures in parallel with PrP121–231 neutralises the toxicity of PrP121–231.[11,13] These biological results show that it is quite possible that potentially toxic regions of the C-terminal domain can be masked by other hydrophobic residues in the rest of the protein and that only an aberrant folding or assembly of the protein exposes them to the environment. Thus, taking into account that the helix II prion domain is a highly competitive anchoring site for copper(II), changes its conformation from α-helix to β-sheet after copper binding, and can interact with artificial membranes, we can speculate that this domain is not normally available to interact with the metal due the masking effect of other regions belonging to the flexible part of the same protein or to other partners. Pathogenic environmental factors, therefore, may facilitate the exposure of physiologically buried copper anchoring sites, thereby triggering abnormal conformational transitions and disease.

Acknowledgements

This work was supported by MIUR (PRIN 2003 031351 and FIRB RBNE01 ARR4-001) as well as by the CNR/MTA bilateral agreement and the Hungarian Scientific Research Fund (OTKA T048352, TS040685 and D048488).

[1] S. B. Prusiner, *Proc. Natl. Acad. Sci. USA* **1998**, *95*, 13363–13383.
[2] P. M Harrison, H. S. Chan, S. B. Prusiner, F. E. Cohen, *Protein Sci.* **2001**, *10*, 819–835.
[3] R. Zahn, A. Liu, T. Luhrs, R. Riek, C. Von Schroetter, F. Lopez-Garcia, M. Billeter, L. Calzolai, G. Wider, K. Wuthrich, *Proc. Natl. Acad. Sci. USA* **2000**, *97*, 145–150.
[4] L. Calzolai, D. A. Lysek, P. G. Guntert, C. Von Schroetter, R. Riek, R. Zahn, K. Wuthrich, *Proc. Natl. Acad. Sci. USA* **2000**, *97*, 8340–8345.
[5] R. P. Bonomo, D. Grasso, G. Grasso, V. Guantieri, G. Impellizzeri, C. La Rosa, D. Milardi, G. Pappalardo, G. Tabbì, E. Rizzarelli, in *Metal Ligand Interactions in Nano-, Micro-, and Macro-Systems in Complex Environments* (Eds.: N. Russo, D. R. Salahub, M. Witko), Kluwer Academic Publishers, Dordrecht, **2003**, pp. 19–36.
[6] C. S. Burns, E. Aronoff-Spencer, C. M. Dunham, P. Lario, N. I. Avdievich, E. E. Antholine, M. M. Olmstead, A. Vrielink, G. J. Gerfen, J. Peisach, W. G. Scott, G. L. Millhauser, *Biochemistry* **2002**, *41*, 3991–4001.
[7] M. Mentler, A. Weiss, K. Grantner, P. Del Pino, D. Deluca, S. Fiori, C. Renner, W. M. Klaucke, L. Moroder, U. Bertsch, H. A. Kretzschmar, P. Tavan, F. G. Parak, *Eur. Biophys. J.* **2005**, 34, 97–112.
[8] R. P. Bonomo, V. Cucinotta, A. Giuffrida, G. Impellizzeri, A. Magrì, G. Pappalardo, E. Rizzarelli, A. M. Santoro, G. Tabbì, L. I. Vagliasindi, *Dalton Trans.* **2005**, 150–158.
[9] D. R. Brown, V. Guantieri, G. Grasso, G. Impellizzeri, G. Pappalardo, E. Rizzarelli, *J. Inorg. Biochem.* **2004**, *98*, 133–143.
[10] M. F. Jobling, X. Huang, L. R. Stewart, K. J. Barnham, C. Curtain, I. Volitakis, M. Perugini, A. R. White, R. A. Cherny, C. L. Masters, C. J. Barrow, S. J. Collins, A. I. Bush, R. Cappai, *Biochemistry* **2001**, *40*, 8073–8084.
[11] G. M. Cereghetti, A. Schweiger, R. Glockshuber, S. Van Doorslaer, *Biophys. J.* **2001**, *81*, 516–525.
[12] S. Van Doorslaer, G. M. Cereghetti, R. Glockshuber, A. Schweiger, *J. Phys. Chem. B* **2001**, *105*, 1631–1639.
[13] G. M. Cereghetti, A. Schweiger, R. Glockshuber, S. Van Doorslaer, *Biophys. J.* **2003**, *84*, 1985–1997.
[14] A. Thompson, A. R. White, C. McLean, C. L. Masters, R. Cappai, C. J. Barrow, *J. Neurosci. Res.* **2000**, *62*, 293–301.
[15] M. Morillas, W. Swietnicki, P. Gambetti, W. K. Surewicz, *J. Biol. Chem.* **1999**, *274*, 36859–36865.
[16] J. D. Harper, P. T. Lansbury, Jr., *Annu. Rev. Biochem.* **1997**, *66*, 385–407.
[17] D. M. Walsh, A. Lomakin, G. B. Benedek, M. M. Condron, D. B. Teplow, *J. Biol. Chem.* **1997**, *272*, 22364–22372.
[18] H. A. Lashuel, L. Zhihong, J. W. Kelly, *Biochemistry* **1998**, *37*, 17851–17864.

[19] M. Anguiano, R. J. Nowak, P. T. Lansbury, Jr., *Biochemistry* **2002**, *41*, 11338–11343.
[20] J. I. Kourie, C. L. Henry, *Croat. Med. J.* **2001**, *42*, 359–374.
[21] M. Salmona, G. Forloni, L. Diomede, M. Algeri, L. De Gioia, N. Angeretti, G. Giaccone, F. Tagliavini, O. Bugiani, *Neurobiol. Dis.* **1997**, *4*, 47–57.
[22] D. Grasso, D. Miliardi, C. La Rosa, E. Rizzarelli, *New J. Chem.* **2001**, *25*, 1543–1548.
[23] D. Grasso, D. Miliardi, C. La Rosa, E. Rizzarelli, *Chem. Commun.* **2004**, 246–247.
[24] D. Grasso, D. Miliardi, V. Guantieri, C. La Rosa, E. Rizzarelli, *New J. Chem.* **2003**, *27*, 359–364.
[25] L. Zékány, I. Nagypál, in *Computational Methods for the Determination of Stability Constants* (Ed.: D. J. Leggett), Plenum Press, New York, **1985**, p. 291.
[26] G. C. Chen, J. T. Yang, *Anal. Lett.* **1977**, *10*, 1195–1207.
[27] D. La Mendola, P. Mineo, E. Rizzarelli, E. Scamporrino, G. Vecchio, D. Vitalini, *J. Supramol. Chem.* **2001**, *1*, 147–151.
[28] P. Mineo, D. Vitalini, D. La Mendola, E. Rizzarelli, E. Scamporrino, G. Vecchio, *Mass Spectrom. Rapid Commun.* **2002**, *16*, 722–729.
[29] T. Heimburg, *Biochim. Biophys. Acta* **1998**, *1415*, 147–162.
[30] I. Sovago, C. Bertalan, L. Gobi, I. Sovago, O. Nyeki, *J. Inorg. Biochem.* **1994**, *55*, 67–75.
[31] R. P. Bonomo, G. Impellizzeri, G. Pappalardo, E. Rizzarelli, G Tabbì, *Chem. Eur. J.* **2000**, *6*, 4195–4202.
[32] R. P. Bonomo, E. Conte, G. Impellizzeri, G. Pappalardo, R. Purrello, E. Rizzarelli, *J. Chem. Soc. Dalton Trans.* **1996**, 3093–3099.
[33] E. Aronoff-Spencer, C. S. Burns, N. I. Avdievich, G. J. Gerfen, J. Peisach, W. F. Antholine, H. L. Ball, F. E. Cohen, S. B. Prusiner, G. L. Millhauser, *Biochemistry* **2000**, *39*, 13760–13771.
[34] J. H. Viles, F. E. Cohen, S. B. Prusiner, D. B. Goodin, P. E. Wright, H. J. Dyson, *Proc. Natl. Acad. Sci. USA* **1999**, *96*, 2042–2047.
[35] A. P. Garnett, J. H. Viles, *J. Biol. Chem.* **2003**, *278*, 6795–6802.
[36] G. Brooks, L. D. Pettit, *J. Chem. Soc. Dalton Trans.* **1975**, 2112–2117.
[37] A. Perczel, M. Hollosi, in *Circular Dichroism and the Conformational Analysis of Biomolecules* (Ed.: G. D. Fasman), Plenum Press, New York, **1996**, pp. 285–380.
[38] M. Luczkowski, H. Kozlowski, M. Stawikowski, K. Rolka, E. Gaggelli, D. Valensin, G. Valensin, *J. Chem. Soc. Dalton Trans.* **2002**, 2269–2274.
[39] D. Valensin, M. Luczkowski, F. M. Mancini, A. Legowska, E. Gaggelli, G. Valensin, K. Rolka, H. Kozlowski, *Dalton Trans.* **2004**, 1284–1293.
[40] G. Di Natale, G. Grasso, G. Impellizzeri, D. La Mendola, G. Micera, N. Mihala, Z. Nagy, K. Õsz, G. Pappalardo, V. Rigó, E. Rizzarelli, D. Sanna, I. Sóvágó, unpublished results.
[41] J. F. Nagle, *Annu. Rev. Phys. Chem.* **1980**, *31*, 175.
[42] K. Basler, B. Oesch, M. Walchli, D. F. Groth, M. P. Mckinley, S. H. White, W. C. Wimley, *Annu. Rev. Biophys. Biomol. Struct.* **1999**, *28*, 319.
[43] G. L. Millhauser, *Acc. Chem. Res.* **2004**, *37*, 79–85.
[44] A. I. Bush, *Trends Neurosci.* **2003**, *26*, 207–214.
[45] B. Belosi, E. Gaggelli, R. Guerrini, H. Kozlowski, M. Luczkowski, F. M. Mancini, M. Remelli, D. Valensin, G. Valensin, *ChemBioChem* **2004**, *5*, 349–359.
[46] C. E. Jones, S. R. Abdelraheim, D. R. Brown, J. H. Viles, *J. Biol. Chem.* **2004**, *279*, 32018–32027.
[47] G. S. Jackson, I. Murray, L. L. P. Hosszu, N. Gibbs, J. P. Waltho, A. R. Clarke, J. Collinge, *Proc. Natl. Acad. Sci. USA* **2001**, *98*, 8531–8535.
[48] B. J. Hathaway, D. E. Billing, *Coord. Chem. Rev.* **1970**, *5*, 143–207.
[49] D. Shmerling, I. Hegy, M. Fischer, T. Blattler, S. Brandner, J. Gotz, T. Rulicke, E. Flechsig, A. Cozzio, C. Von Mering, C. Hangartner, A. Aguzzi, C. Weissmann, *Cell* **1998**, *93*, 203–214.

Received: May 13, 2005
Published online: September 15, 2005

